

CORROSION BEHAVIOUR OF TRIP STEELS IN DIFFERENT NaCl SOLUTIONS

Animesh Talapatra,
Lecturer, Dept.of automobile engg,
MCKV Institute of engineering, Howrah-711204,India

Abstract: Corrosion behaviours of two moderately low carbon high strength low alloy steels designated as A (having no Cr and Cu content) and B (having higher Ni , Cr and Cu content) heat treated at different condition to alter micro-structure phases, have been studied under the simulated condition of marine atmosphere in the laboratory scale in different level of salinity under the influence of neutral pH as well as exposing them in real sea water condition by using electro-chemical test . Pre and post corrosion micro-structural studies and quantitative phase analysis were carried out to arrive at structure-schometry-corrosion co-relation for designing of steels for naval application.

Keyword: Corrosion; Trip steels; Electrochemical measurements; Phase analysis.

1 . INTRODUCTION:

Development of newer types of low alloy high strength corrosion resistance steel has been attempted by many researchers all over the world for marine application [1-5]. It has been reported that major factors those effect the corrosion rate of such low alloy high strength steel are

- i) Chemical composition
- ii) Composition of sea water
- iii) Type of exposures and supply of O₂ in corroding interface. Corrosion process for steel in seawater is controlled by anodic and cathodic reaction.
 - a) The anodic reaction is: Fe.... Fe²⁺ +2e⁻
 - b) In seawater, oxygen reduction is the cathodic reaction.



Corrosion continues till surface is enriched with phases having Cu, Ni and Cr. Accumulation of Cu, Ni & Cr phases at the surface causes a depolarisation in cathodic reaction but polarize anodic reaction (5-6). The alloy elements such Cu, Ni, Al, Mn, Mo etc. has been seen to provide pronounced effect during atmospheric corrosion of steel. In the seawater condition however their rule had been reported to depend on the length of the exposure of the material in the electrolyte. Ni –base alloys containing Cr and Fe are very resistant to flowing seawater, but in stagnant or very low velocity seawater pitting or crevice corrosion can occur.

In moderate-velocity and high velocity seawater or brackish water, Ni base alloy is frequently used for pumping .It has excellent resistance to cavitations erosion and exhibits corrosion rates of less than 0.025 mm/year. Other Ni-base alloys containing Cr and Mo offer increased resistance to localized corrosion in stagnant seawater.

Seawater is a highly conductive environment with approximately 3.4% salt (NaCl) concentration (3-6). Other factors that contribute to the corrosivity of seawater include oxygen concentration, velocity, temperature, and pressure of marine biological species. Seawater contains about 35g dissolved salts per 1kg of seawater where the dissolved salts have the following composition by weight: 77.76 %NaCl, 10.88%MgCl, 4.74%MgS₄ (magnesium sulphite), 3.60% CaS₄ (Calcium Sulphite), 2.46% KCl, 0.22%MgBr₂ (Magnesium bromide), 0.34% CaCO₃. Approximately 91.1% of the dissolved salts are chlorides. There are other commonly occurring constituents, dissolved gases, living organisms and various other materials found in seawater. Rivers, temperature, dissolved oxygen, and pollutants are some examples of issues that may affect the corrosion of a given component in seawater.

Keeping in view above study on corrosion behaviors to moderately low carbon steel having Si, Mn, Ni, V, Nb, Mo and/or Cu and Cr, designed and develop for naval application has been attempted in this study. Electro-chemical test under simulated condition of marine atmosphere both at laboratory stage and real seawater condition, beside immersion test by varying the control parameters viz. exposure time, influence of pH, salinity etc. are the methodology that would be adopted for evaluation of corrosion characteristics. No database being available in literature on the systematic study on effect of corrosion on multi-phases microstructure efforts are being made to find out a correlation with post and pre-corrosion microstructure with corrosion behaviour of the steels.

2. LITERATURE REVIEW

Development corrosion resistance steel for marine application is the on-going research all over the globe. From various literatures, it is seen that improvement of steel's microstructure, its physical and mechanical properties does not give complete solution for corrosion resistance in sea atmosphere. Though some steels have given better microstructure for corrosion resistance, but it's physical or mechanical properties are not suitable.

Juan J. Santana Rodriguez, F. Javier Santana Hernandez, (Corrosion Science 45 (2003), 799-815), who worked on atmospheric corrosion of carbon steel, observed that Cl^- ions with SO_2 only being of significance in sea area corrosion. This Cl^- ions are also responsible for increasing in diameter of pitting.

P. Ernst, R. C. Newman, (Corrosion Science, 44 (2002), 943-954), worked one the effect of temperature, chloride concentration and sulphate addition on pit growth. They observed that the formation of a lacy metal cover is necessary to maintain stable pit growth, pit shape, morphology and cover formation in dilute NaCl solutions are influenced by the solution resistivity.

Hou Baorong and Xiang Bin (Bull Mater. Sci., Vol. 26, No. 3, Indian Academy of Science), worked on corrosion for marine structural steel, observed that the rust layer components appearance and corrosion type of the Ni-Cu-P steel specimens due to general corrosion, pitting corrosion in various zone.

E. Sosa, M. T. Oropeza, I. Garcia, (Corrosion Science, 44 (2002), 1515-1528) worked on surface damage in corrosion process. They observed diffusion processes of Fe^{2+} and H^0 ions through the corrosion product film.

Literature survey indicates that considerable efforts are being made all over the world to develop newer types of low alloy high strength corrosion resistance steels for Marine Application [1-5]. Prior to the development of high strength low-alloy (HSLA) steels, ferrite - pearlite and quenched and tempered steels were used in structures where high strength was required. The former steels also known as high tensile steels (HTS) have moderate strength (350MPa) and obtained strength through pearlite strengthening by the addition of carbon upto 0.2%. In 1960's quenched and tempered (Q and T) steels were developed to improve the performance of structural components in Naval Applications. The strength of these steels also depended on carbon. Due to higher carbon contents ($> = 0.2\%$), these steels suffer from poor weldability and therefore, the need for the development of steel with improved weldability and appropriate hardenability were felt. To achieve higher yield strength, higher resistance to brittle fracture as well as low transition temperature and improved weldability, new classes of steels having very low carbon contain and higher alloying elements were developed.

3.EXPERIMENTAL PROCEDURE

3.1 Materials

Two moderately low carbon high strength low alloy steels for marine application designated as A and B having composition given in Table 1 were supplied DMRL.

TABLE –1

CHEMICAL COMPOSITION

	C	Mn	Si	P	Ni	Cr	Cu	V	Nb	Mo
A	0.11	1.35	0.32	0.024	0.75	-	-	0.03	0.03	-
B	0.10	0.47	0.28	0.022	2.02	0.40	0.60	0.03	-	0.44

3.2 Heat treatment

Steels were heat-treated as per schedules shown in below to develop different microstructures:

STEEL	SCHEDULE NO.	HEAT -TREATMENT	DESIGNATION
A	1	As received (oil quenched and tempered)	A1
	2	Held at 950°C for 1/2hr, air cooled, Held at 700°C for 2 hrs, quenched to 400°C(salt bath), held for 900s and oil quenched.	A2
	3	Held at 950°C for 1/2hr., oil quenched in an oil of viscosity 0.123 centistokes.	A3
	4	Held at 950°C for 1/2hr., then cooled in water.	A4

	5	Held at 950°C for 1/2hr., then cooled in air.	A5
	6	Held at 950°C for 1/2hr., then cooled in furnace by switching off	A6
B	1	As received (water quenched and tempered)	B1
	2	Held at 970°C for 1/2hr, air cooled, Held at 800°C for 2 hrs, quenched to 400°C(salt bath), held for 900s and oil quenched.	B2
	3	Held at 970°C for 1/2hr., oil quenched in an oil of viscosity 0.123 centistokes	B3
	4	Held at 970°C for 1/2hr., then cooled in water.	B4
	5	Held at 970°C for 1/2hr., then cooled in air	B5
	6	Held at 970°C for 1/2hr., then cooled in furnace by switching off.	B6

3.3 Optical micrography

The micro structural characterizations of the steels were carried out using an OLYMPUS CK4OM-CP optical microscope. The optical metallography of all these samples were carried out in the usual way. Samples were cut from plates of these steels. These samples were polished on polishing wheel after 1 to 6 (rough to fine) emery papers. The polished surface appeared like mirror having no scratches and the etchant was used 2% nital. The washed and dried samples were observed carefully in Microscope at different magnifications and some selected photomicrographs were taken.

3.4 PHASE ANALYSIS

The phase analyses have been done by using Olysia m3 software. Samples were prepared as like as preparation of sample for optical microscope observation. Then images were taken in optical microscope. The acquired images of a multi-phase object were taken to analyse. Phase analysis will be conducted on a gray-value image. The image is selected and threshold is set to define the gray value ranges for the separate phases. The OLYSIA software created a measurement sheet showing the absolute area and proportional area (in %) of all the phases. The measured values are taken.

3.5 ELECTRO-CHEMICAL STUDY:

SAMPLES AND SOLUTION PREPARATION:

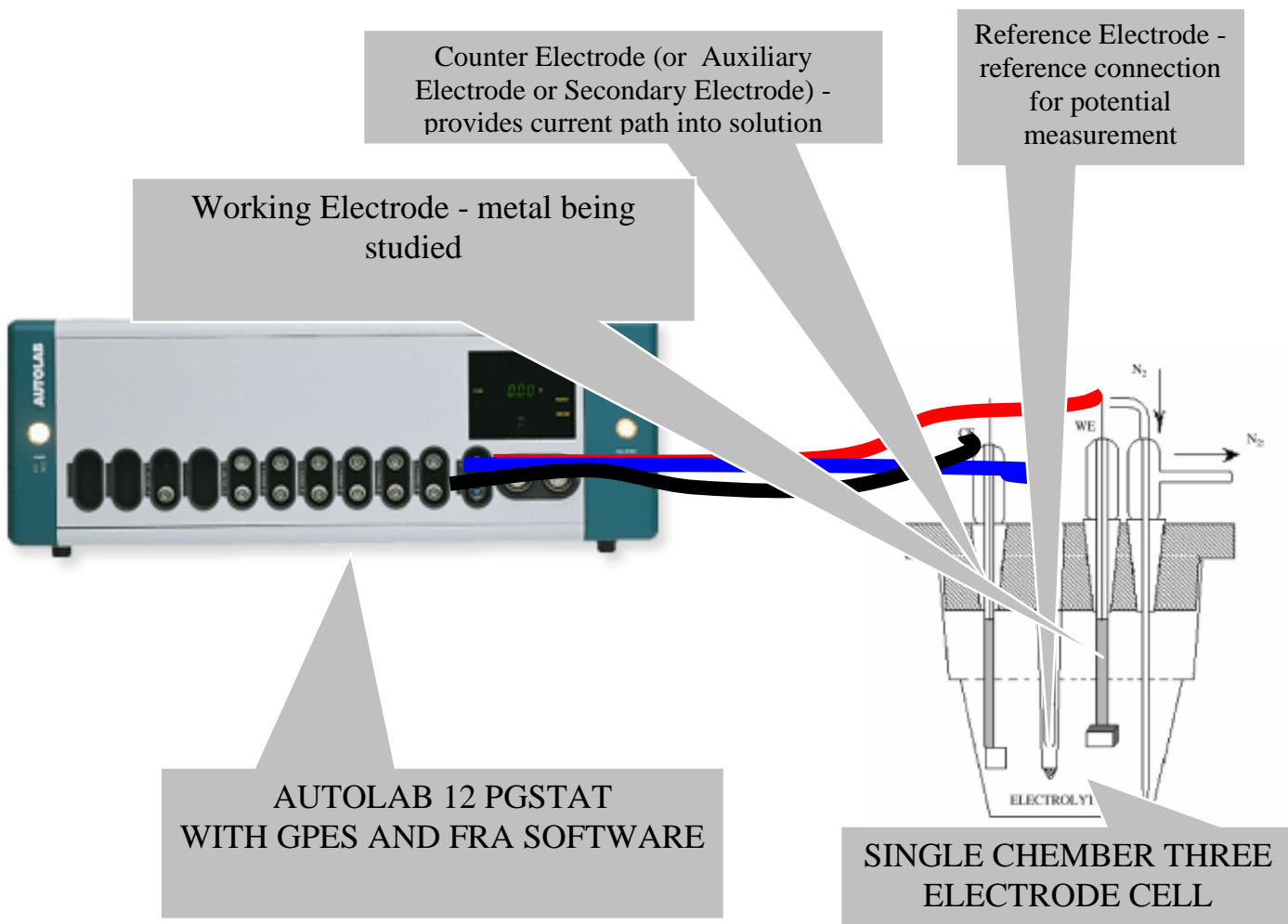
Samples were cut from plates of these steels. These samples were polished on belt followed by polishing on polishing wheel with 1 to 6 (rough to fine) emery papers. The polished surface appeared like mirror having no scratches. They were then degreased with acetone before exposing to the electro-chemical test. Solution of 0%, 0.1%, 1% and 3% NaCl at pH 6.5 were prepared with triple distilled water.

POLARIZATION STUDY: samples were taken in an area of 0.204 cm^2 ($0.40 \text{ cm} \times 0.51 \text{ cm}$) size coupons for performing potentiodynamic polarization studies in de-aerated condition in cells with three electrode configuration and using aqueous saturated calomel SCE (W) ($E^0=0.24 \text{ V vs. SHE}$) as the reference electrode and Pt foil as counter electrode. Linear sweep voltammetry was performed with the help of AUTOLAB 12 PGSTAT, Eco Chemie B.V (the Netherlands) at 0.5 mv/s scan rate within the potential range of -1500mv to the cathodic potential of 650mv vs. SCE. Potential scans were conducted in de-aerated conditions by purging the solution with N_2 for 10 mines. Tafel analysis was performed to determine the corrosion parameters. Result of the polarization study has given in the (table-3 to table-6) and corresponding bar chart has shown in (fig-66 to fig-81).

ELECTRO-CHEMICAL IMPEDANCE SPECTROSCOPY STUDY: EIS at the respective OCP value were recorded with the help of AUTO-LAB 12 PG STAT, Eco Chemie B.V (the Netherlands). Combined with frequency response analyzer (FRA) module. The sinusoidal perturbation of 5mv amplitude was applied at the cell over the frequency range of 100 kHz to 10 MHz. EIS measurements were conducted at open

circuit conditions after a steady state potential was attained in aerated solution of different electrolytes at neutral pH. The experiment was performed in a three -electrode one compartment cell containing the test coupons as the working electrode, a large area Pt foil as counter electrode and a saturated calomel reference. Result of this study has shown in (fig-60 to fig-65).

SETUP OF ELECTRO-CHEMICAL EXPERIMENTS



4. RESULT AND DISCUSSION

MICROSTRUCTURAL CHARACTERISTIC

The optical microstructure (fig-8) of steel A heat-treated at schedule A1 reveals mostly polygonal ferrite with certain amount of tempered bainite. The optical microstructure (fig-18) of steel B in condition B1 reveals mostly tempered bainitic structure with certain amount of blocky polygonal ferrite.

When the A steel was subjected to intercritical annealing followed by quenching in salt bath for incomplete bainitic transformation, following the conventional heat-treatment schedule of TRIP aided dual phase steel (A₂), the microstructure (fig-10) is, as expected, consist of granular ferrite and bainite. The microstructure of the steel continuously cooled with increasing cooling rate (A₃) i.e. decrease in viscosity of the quenching medium, has increased the acicularity of the microstructure (fig-12). The microstructures comprise of mostly acicular ferrite/bainite with certain amount of quasi-polygonal and granular ferrite.

When the steel B was heat-treated, the microstructure (fig-20) is found to be consisting of acicular ferrite/bainite with some islands of polygonal and quasi-polygonal ferrite (B₂). The microstructure (fig-22) of the steel continuously cooled with increasing cooling rate (B₃) comprise of low temperature transformation product of austenite, mostly acicular ferrite/bainite with some amount of granular ferrite. Increase in cooling rate has increased the acicularity of the microstructure with some amount of martensite laths.

Further A and B steel was heat treated at schdule A4, A5, A6, and B4, B5, B6. The microstructure

of those steels reveal, martensite, ferrite and retain austenite (for schedule A4) as shown in fig-14, coarse pearlite, retain austenite and ferrite (For A 5) as shown in fig-16, ferrite, austenite and pearlite /bainite (in A 6) as shown in fig-18. In case of steel B microstructures reveal martensite, ferrite and retain austenite (for schedule B 4) as shown in fig-26, coarse pearlite, retain austenite and ferrite (For B5) as shown in fig-28, ferrite, austenite and pearlite /bainite (in B 6) as shown in fig-30.

All the above microstructure when subjected to image analyzing system and volume fraction of phase present in structure are determined (Table-2). While the in the conventionally heat treated A4, A5, A6 and B4, B5, B6 volume fraction of phases of the microstructure maintained its typical behaviour of high % of martensite and/or pearlite in ferrite matrix during water and air cooling, incase of furnace cooling / annealing volume fraction of ferrite is found to be higher due to obvious reason. In case of other microstructures of both steels heat treated at different schedules having multi-phases, primarily reveal the higher percentage of nonequilibrium phases according to rate of cooling. Two major phases, in such cases, are broadly considered for further co-relation with corrosion behaviour.

POST CORROSION MICROSTRUCTURE

Post corrosion microstructures, taken for a few samples for both steels, reveal adequate corrosion both in the form of grain boundary attack and pitting. However steel having high percentage of Cu and Cr, in case of steel B, this corrosion attack is comparatively less in all heat treatment schedules seemingly due to formation of protective oxide layer. Post corroded microstructures of samples are shown in (fig-32 to fig-47).

CORROSION CHARACTERISTIC

Typical polarisation plots as shown in (Fig-50 and Fig-51) of A2 and B2 in 0.1% NaCl shows that B2 is characterized with a narrow but distinct passive region while in A2 there is no such region. EIS measurement reveals the Nyquist plot as shown in (Fig-60 to Fig-65) where the diameter of half-circles represent the circuit resistance of the material. While in pure water (0% NaCl) Nyquist plots as shown in (Fig-64 and fig-65) are characterized with two subsequent but overlapping semicircles, in Cl⁻ ions containing solution only single half-circles are obtained. In neutral pH when EIS represents dual character A samples are more resistant than B samples $R_p(A) > R_p(B)$. It may be predicted that matrix / grain boundary of A is more reactive than that of B in neutral conditions and that may be due to formation of thicker and stern passive layer (oxide film) in alloy B. This gets disrupted immediately in contact with Cl⁻. In most of A and B samples 10-fold decrease is observed when exposed to 0.1% NaCl. However this decrease is much restricted in case of B2 and B3 samples. With further increase in Cl⁻ ion R_p decrease as usual. A more or less similar behavior is reflected with polarization studies. Corrosion current/corrosion rate are much higher for A samples than B ones. Increase in Cl⁻ ion concentration increases the corrosion rate in both samples. Interestingly enough, in case of B2 and B3 samples corrosion rates are not that significantly accelerated with [Cl⁻] as in case of A samples. In the contrary, B2, B3 sample exhibits resistant behavior when polarized in 0.1%, even more than when studied in 0% NaCl. This in fact translates to a dual influence of oxidation kinetics and film repair process in the mild Cl⁻ concentrations.

CORROSION –MICROSTRUCTURE –PHASE PROPERTY CO-RELATION

Alloy A when water quenched from the austenitic region A4 was found that microstructure contains around 73% martensite. When the same alloy was normalized (A5), the amount of the second phases was found to be higher but the corrosion behavior of the normalized sample was found to be greater than the alloy in quenched condition (water). This may be due to fact that the amount of nonequilibrium phases in A4 is much higher than A5. As the second phase in A5 may contain with some amount of bainite and mostly pearlite. When the alloy was annealed the amount of ferrite increases considerably and the second phase being pearlite. When the alloy was heat-treated accordingly schedule 2 and 3 the microstructure predominantly consists of ferrite and bainite with certain possibility of presence of martensite-austenite (MA) constituent. Though the phase analysis shows a comparable phase distribution A2 and A3, general acicularity of A3 microstructure is definitely higher and hence corrosion rate for A3 was also higher though marginally. A1 sample is quenched and tempered directly from the hot rolled condition. Though the amount of second phases presence in microstructure is lower than A2 and A3, corrosion result shows that it has least corrosion resistance in this particular condition. This may be due to presence of high density of dislocation in microstructure, which is not possible to reveal in the microscopy made in this work.

Incase of alloy B similar phenomenon could be observed in almost all the heat treated condition. Here also B6 shows the most corrosion resistance property compared to other sample. Incase of B2 and B3, like alloy A, corrosion results are comparable, B3 showing A marginally lesser corrosion resistance particularly at lower concentration of NaCl. Here also it is found that B1 is the most corrosive in nature and this may also be attributed has to presence of dislocation in the microstructure. It is generally found that

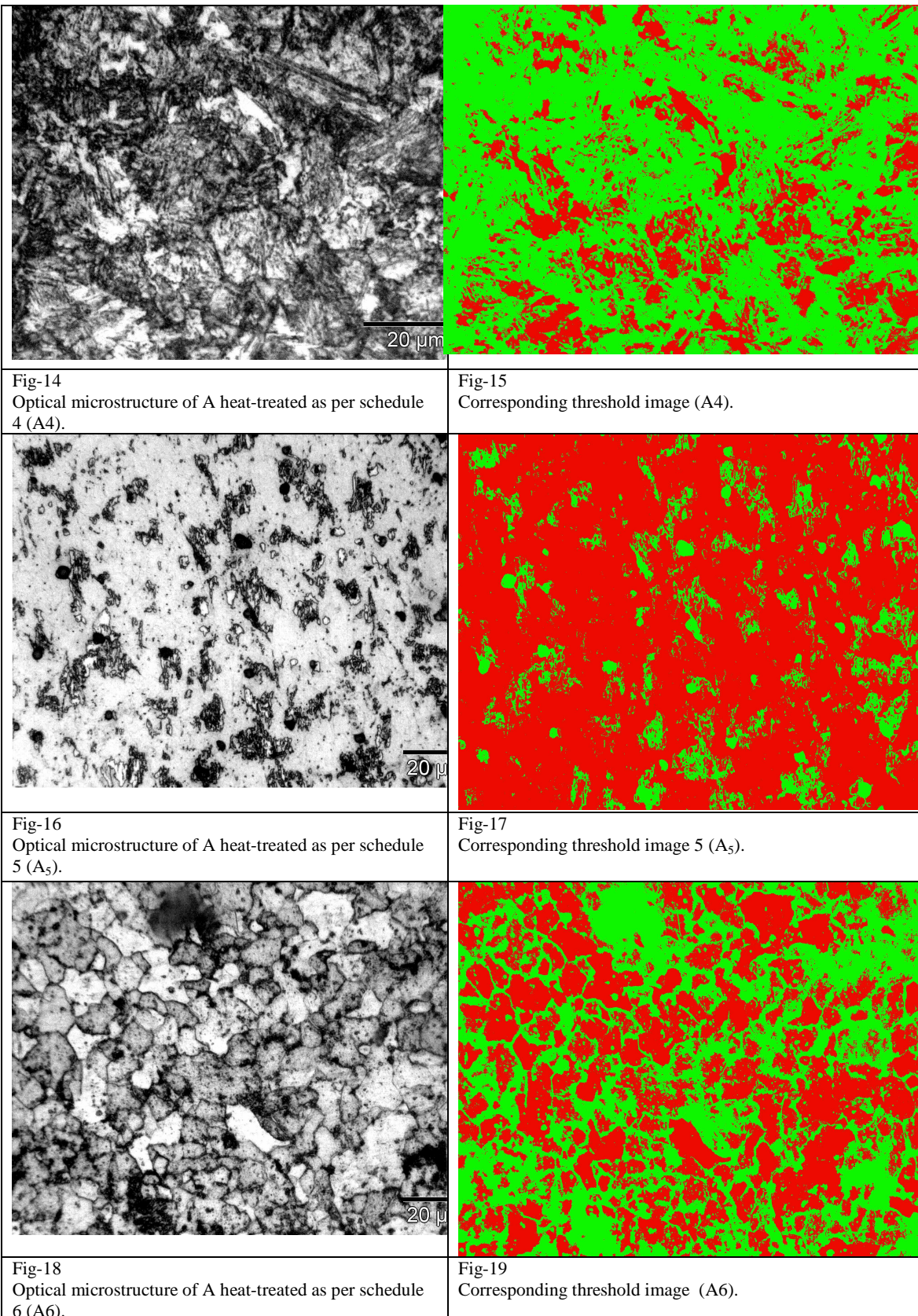
alloy B has superior corrosion resistance property than alloy A when compared at any particular heat treatment condition. This is probably due to presence of Cr and Cu in alloy B. The steel shows the highest corrosion resistance property. This is due to the presence of equilibrium phases in the microstructure.

5. Conclusion

1. As high-energy regions are prone to corrosion, microstructure having finer grains, that is more grain boundary, has less corrosion resistance.
2. Microstructure contains more low temperature transformation products like bainite and/or martensite and other nonequilibrium are more corrosion.
3. Steel containing more Cu, Ni and Cr is less corrosive compared to other steels having same processing or microstructure.
4. Steels in rolled condition are more corrosive in both the case, probably due to high dislocation density.

6 . REFERENCES

1. I.Yu.Konnva, T.K. Sergeeva, V.G.Gontmakher, N.A.Pavienko, Sov.Mat.Sci. Rev. 3 (1-4), (1989) 243,456
2. E.Anelli,L.CaribaniandA.Mascanzoni,Abstract: Processing, Microstructure and properties of HSLA steels, TMS/AIMS, 420, Pensilvania, 1086 (1988)
3. F. Blekkenhorst, G. M. Ferrari, C. J. Van Der Wekkan and F. P. Ijsseling, Brit. Corrosion., J. 21 (1986) 163
4. G. Thomas, LCFA-92, Jamshedpur, India, March 1992
5. Ernest J. Czryca, Richard E. Link, R. J. Wang, D. A. Aylor, T. W. Montemarano and J. P. Crudas, Naval Engineering J, May 1990) 63.
6. W.A. Schultze and C. J. Van Der Wekken, Brit. Corrosion J., 11 (1976) 18
7. C. Wagner, J. Electrochem Soc., 103 (1956) 571.
8. D. D. N. Singh, A. K. Dey, Mahuya Dey and B. K. Singh (unpublished work)
9. G. Thomas, LCFA-92, Jamshedpur, India, March 1992
10. I. Yu Konnva, T. K. Sergeeva, V. G. Gontmakher, N. A. Pavienko, Sov. Mat. Sci. Rev., 3 1-4), (1989) 243
11. F. Blekkenhorst, G. M. Ferrari, C. J. Van Der Wekken and F. P. IJSSELing, Brit. Corrosion. J., 21(1986) 163
12. Ernest J. Czyreca, Richard E. Link, R. J. Wang, D. A. Aylor, T. W. Montemarano and J. P. Crudas Naval Engineering J. May (1990) 63
13. C. Wagner J. Electrochem. Soc., 103 (1956) 571
14. Baorong Hou 1981 Studia Marine Sinica 1887
15. Baorong Hou et al 2002 Mater. Perf. 42.2
16. Schumacher M 1979 Sea Water Corrosion hand book (New Jersey, USA: Noyes Data Corporation) p.12
17. G. OISEN, "Computational Design of Hierarchically Structured Materials", Science 277, 1237-1242 (1997)
18. H. Herman, S. Sampath, R. McCune, MRS Bull (2000) 17



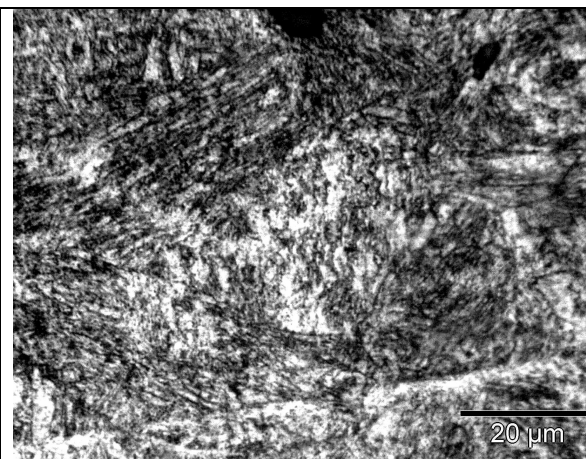


Fig-26
Optical microstructure of A heat-treated as per schedule 4 (B4).

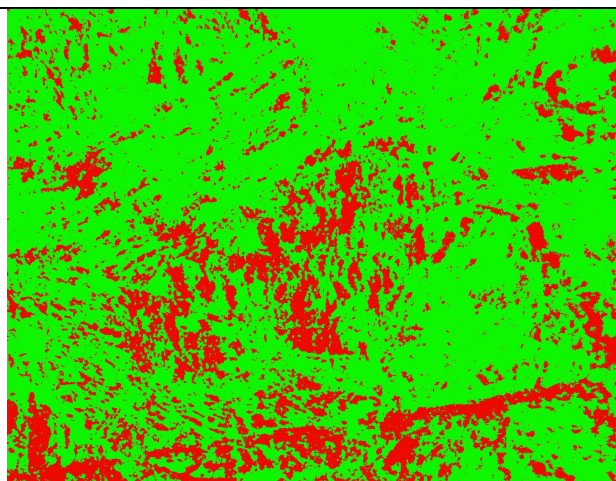


Fig-27
Corresponding threshold image 4 (B4).

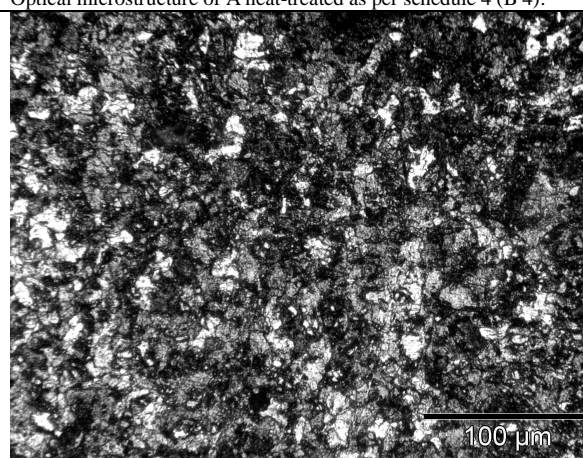


Fig-28
Optical microstructure of A heat-treated as per schedule 5 (B5).

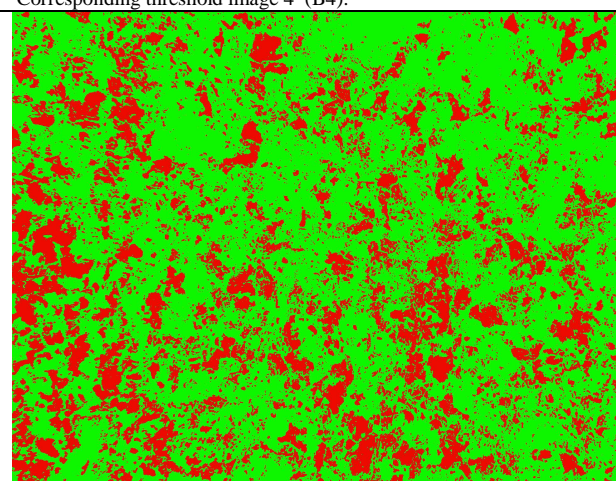


Fig-29
Corresponding threshold image 5 (B5).

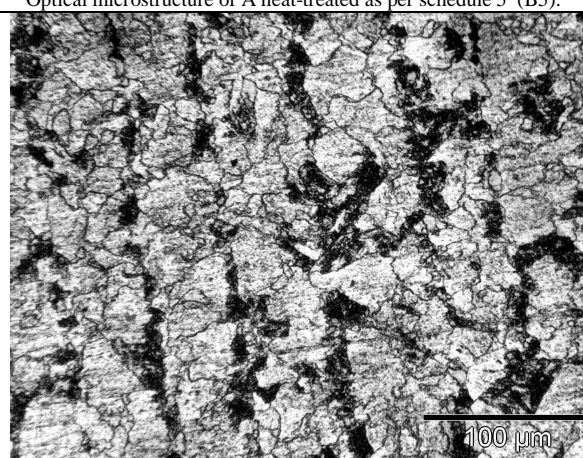


Fig-30
Optical microstructure of A heat-treated as per schedule 6 (B6).

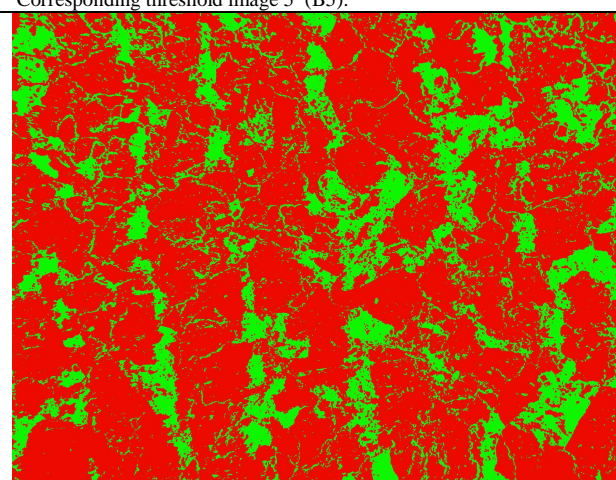


Fig-31
Corresponding threshold image 6 (B6).

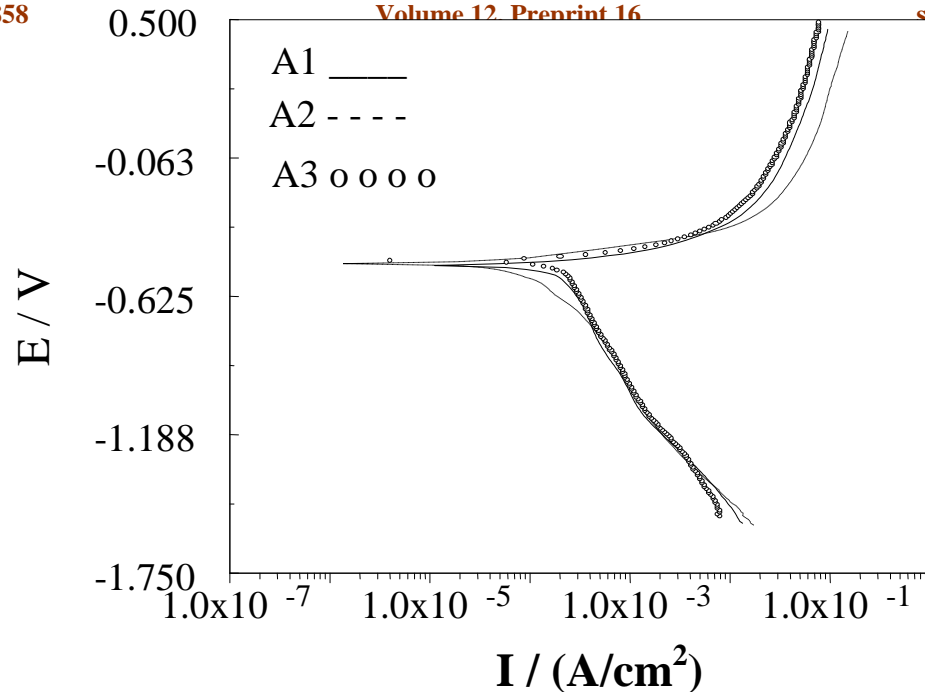


Fig-54: Polarisation plot for Corrosion studies in 1%NaCl at neutral pH. Alloys A1, A2 and A3

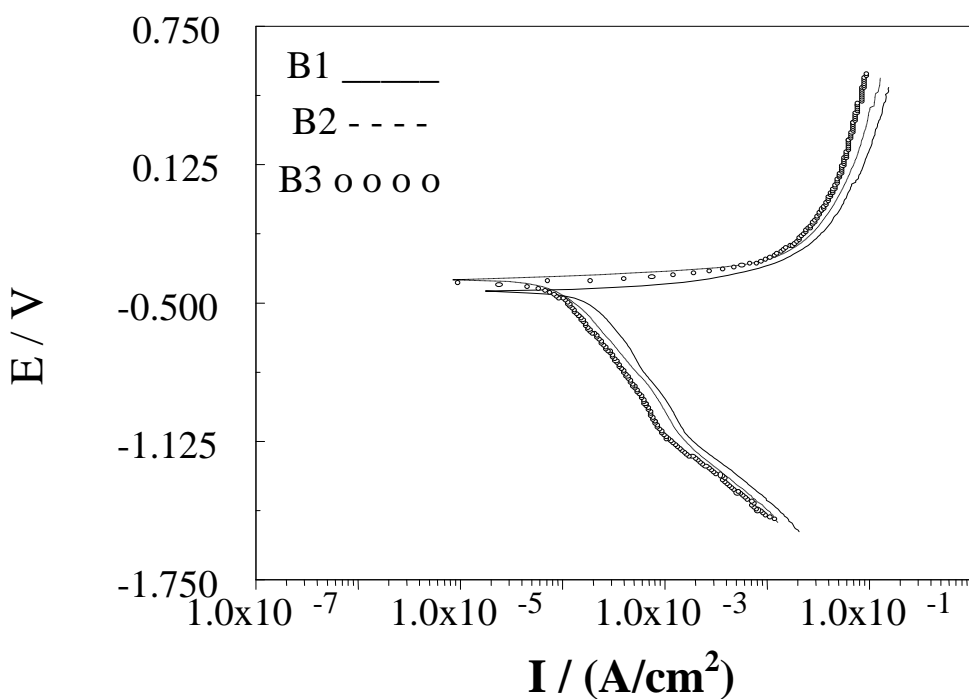


Fig-55: Polarisation plot for Corrosion studies in 1%NaCl at neutral pH. Alloys B1, B2 and B3

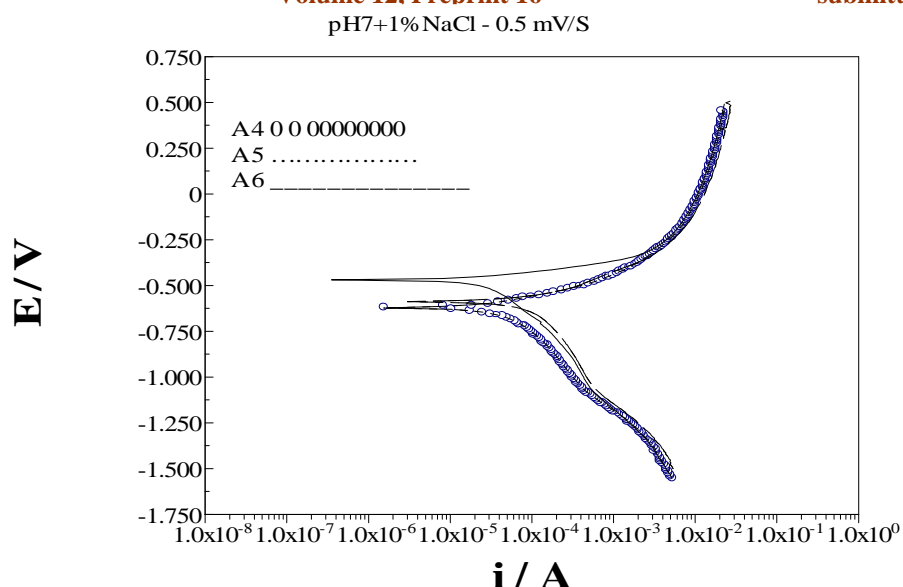


Fig-56: Polarisation plot for Corrosion studies in 1%NaCl at neutral pH. Alloys B4, B5 and B6

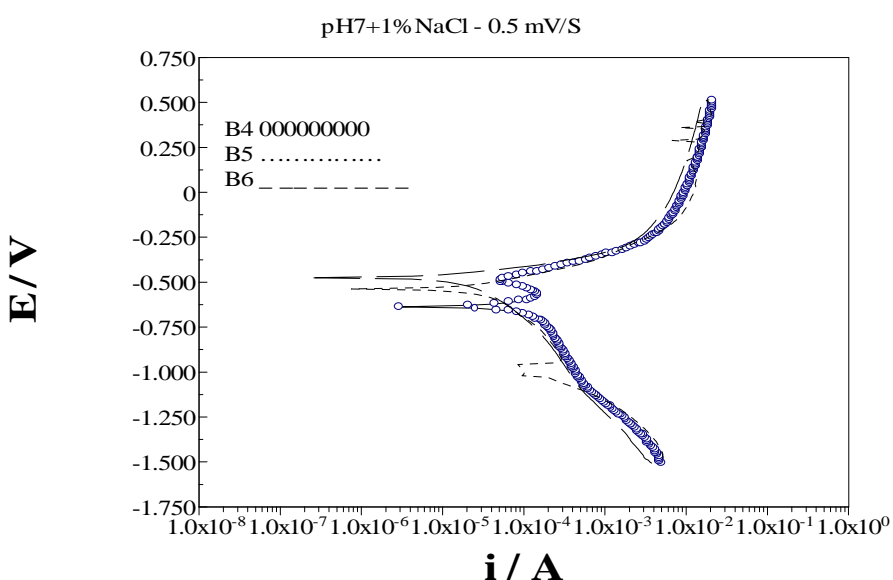


Fig-57: Polarisation plot for Corrosion studies in 1%NaCl at neutral pH. Alloys B4, B5 and B6

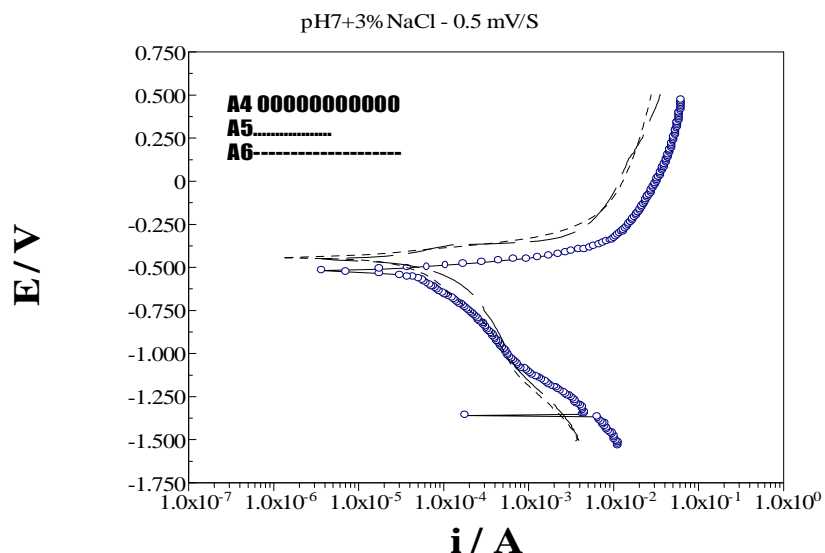


Fig-58: Polarisation plot for Corrosion studies in 3% NaCl at neutral pH. Alloys A4, A5 and A6

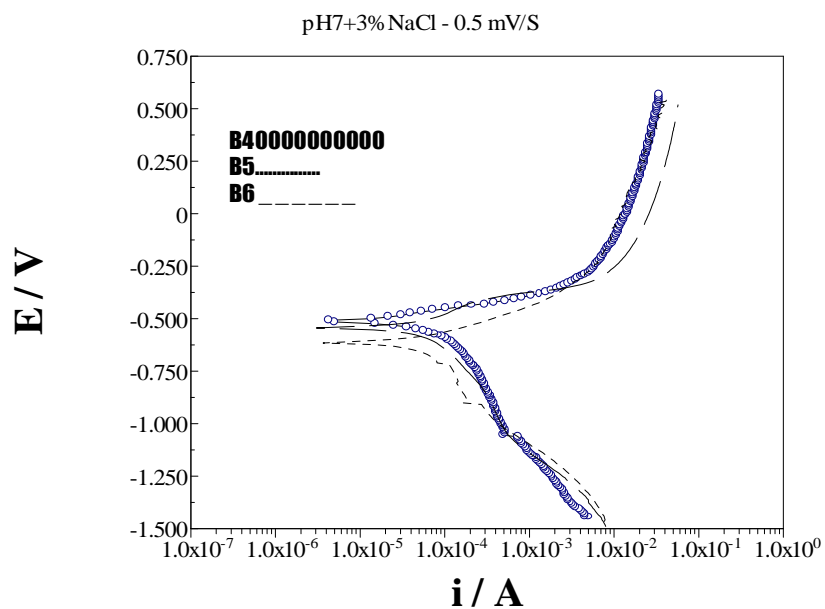


Fig-59: Polarisation plot for Corrosion studies in 3% NaCl at neutral pH. Alloys B4, B5 and B6

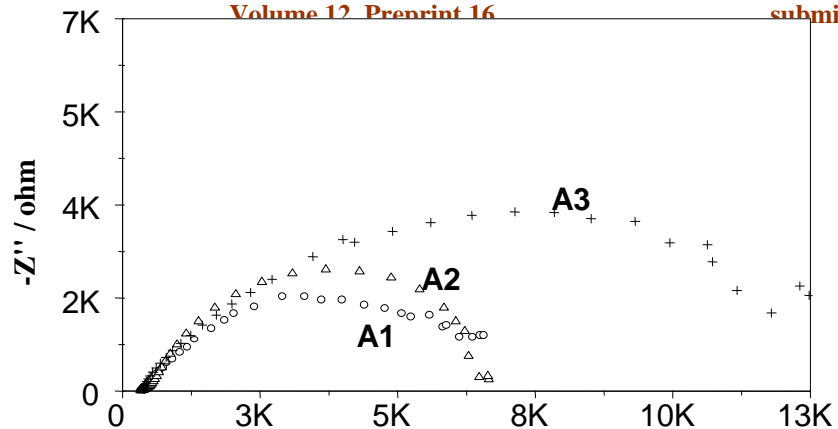


Fig-60: 0.1% NaCl - Nyquist plot for A1, A2 and A3

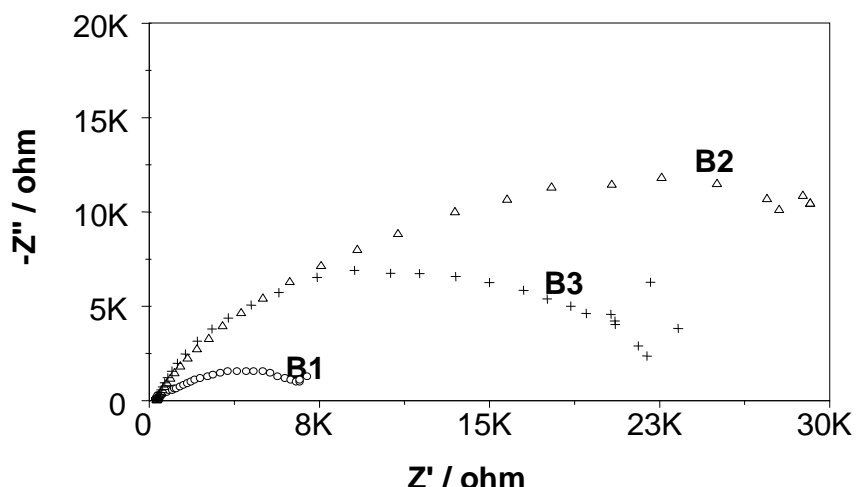


Fig-61: 0.1% NaCl - Nyquist plot for B1, B2 and B3

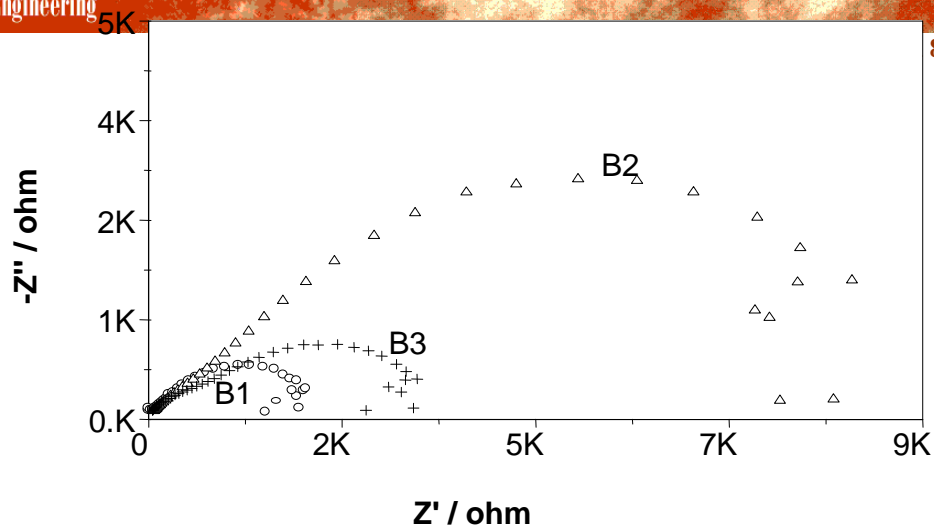


Fig-63: 1% NaCl - Nyquist plot for B1, B2 and B3

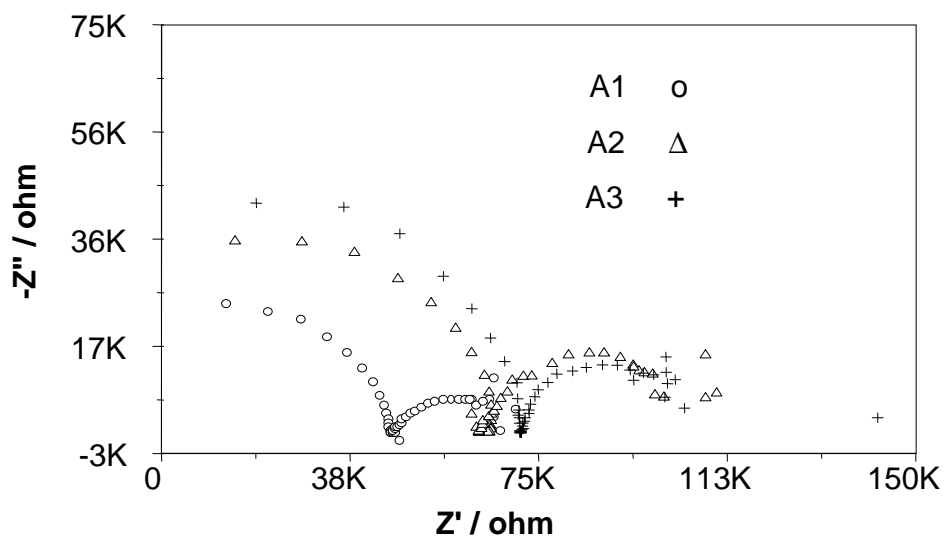


Fig-64: 0% NaCl - Nyquist plot for A1, A2 and A3

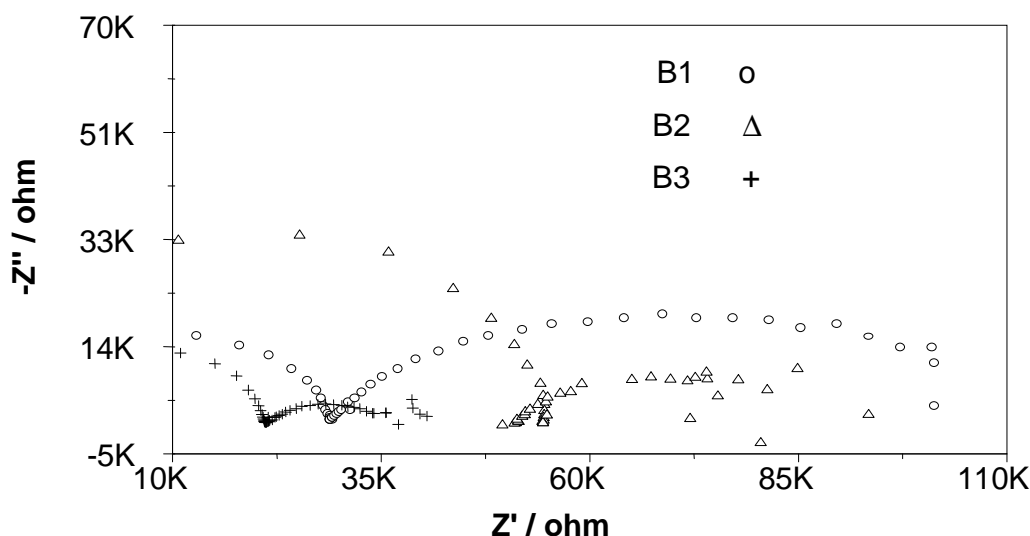


Fig-65: 0 % NaCl - Nyquist plot for B1, B2 and B3

TABLE-2: Volume fraction of micro structural phases of steel A and B

SAMPLE	FERRITE	TEMPERED BAINITE	BAINITE	PEARLITE	MARTENSITE
A1	70.617	29.382			
A2	46.515		53.484		
A3	52.485		47.514		
A4	26.964				73.035
A5	13.975			86.024	
A6	52.255			47.744	
B1	43.117	56.882			
B2	50.675		49.324		
B3	56.561		43.438		
B4	23.855				76.144
B5	29.177			70.822	
B6	75.220			24.779	

TABLE-3 CORROSION POTENTIAL

SAMPLE	PARAMETER	0%NaCl	0.1%NaCl	1%NaCl	3%NaCl
A	A ₁	E _{corr} (Volt)	-0.424	-0.391	-0.503
	A ₂	E _{corr} (Volt)	-0.378	-0.404	-0.490
	A ₃	E _{corr} (Volt)	-0.406	-0.416	-0.480
	A ₄	E _{corr} (Volt)		-0.398	-0.621
	A ₅	E _{corr} (Volt)		-0.384	-0.585
	A ₆	E _{corr} (Volt)		-0.291	-0.467
B	B ₁	E _{corr} (Volt)	-0.360	-0.356	-0.448
	B ₂	E _{corr} (Volt)	-0.453	-0.324	-0.391
	B ₃	E _{corr} (Volt)	-0.341	-0.397	-0.417
	B ₄	E _{corr} (Volt)		-0.442	-0.520
	B ₅	E _{corr} (Volt)		-0.397	-0.468
	B ₆	E _{corr} (Volt)		-0.321	-0.355

TABLE-4 CORROSION CURRENT

SAMPLE	PARAMETER	0%NaCl	0.1%NaCl	1%NaCl	3%NaCl
A	A ₁	I _{corr} $\frac{2}{2} \frac{5}{5}$ (A/Cm ²) X 10 ⁻⁵	4.7	7	71
	A ₂	I _{corr} $\frac{2}{2} \frac{5}{5}$ (A/Cm ²) X 10 ⁻⁵	1.4	3.6	27.2
	A ₃	I _{corr} $\frac{2}{2} \frac{5}{5}$ (A/Cm ²) X 10 ⁻⁵	1.5	5.8	44.7
	A ₄	I _{corr} $\frac{2}{2} \frac{5}{5}$ (A/Cm ²) X 10 ⁻⁵		3.127	9.378
	A ₅	I _{corr} $\frac{2}{2} \frac{5}{5}$ (A/Cm ²) X 10 ⁻⁵		2.207	7.081
	A ₆	I _{corr} $\frac{2}{2} \frac{5}{5}$ (A/Cm ²) X 10 ⁻⁵		1.143	5.518
B	B ₁	I _{corr} $\frac{2}{2} \frac{5}{5}$ (A/Cm ²) X 10 ⁻⁵	2.4	2.3	93.6
	B ₂	I _{corr} $\frac{2}{2} \frac{5}{5}$ (A/Cm ²) X 10 ⁻⁵	2.9	1.9	10
	B ₃	I _{corr} $\frac{2}{2} \frac{5}{5}$ (A/Cm ²) X 10 ⁻⁵	4.7	3.9	9.2
	B ₄	I _{corr} $\frac{2}{2} \frac{5}{5}$ (A/Cm ²) X 10 ⁻⁵		2.812	8.288
	B ₅	I _{corr} $\frac{2}{2} \frac{5}{5}$ (A/Cm ²) X 10 ⁻⁵		2.511	7.400
	B ₆	I _{corr} $\frac{2}{2} \frac{5}{5}$ (A/Cm ²) X 10 ⁻⁵		1.418	3.269

TABLE-5 POLARISATION RESISTANCE

SAMPLE	PARAMETER	0%NaCl	0.1%NaCl	1%NaCl	3%NaCl
A	A ₁ R _P (Kohm)	47.5	4.36	2.2	0.35
	A ₂ R _P (Kohm)	66.7	5.2	1.1	0.35
	A ₃ R _P (Kohm)	74	7.3	0.9	0.43
	A ₄ R _P (Kohm)		1.041	0.359	0.159
	A ₅ R _P (Kohm)		1.309	0.4466	0.2482
	A ₆ R _P (Kohm)		1.39	0.8242	0.3559
B	B ₁ R _P (Kohm)	31.5	3.5	1.3	0.6
	B ₂ R _P (Kohm)	55.3	20.1	5.5	1.2
	B ₃ R _P (Kohm)	23	16.5	1.2	0.4
	B ₄ R _P (Kohm)		0.7162	0.4747	0.1584
	B ₅ R _P (Kohm)		1.913	0.5354	0.2858
	B ₆ R _P (Kohm)		2.226	1.084	0.5161

TABLE-6 CORROSION RATE

SAMPLE	PARAMETER	0%NaCl	0.1%NaCl	1%NaCl	3%NaCl
A	A ₁ CR (mm/yr)	0.361	0.539	5.467	
	A ₂ CR (mm/yr)	0.107	0.277	2.094	
	A ₃ CR (mm/yr)	0.1155	0.4466	3.4419	
	A ₄ CR (mm/yr)		0.351	2.704	1.076
	A ₅ CR (mm/yr)		0.2477	1.313	1.066
	A ₆ CR (mm/yr)		0.1283	0.619	0.874
B	B ₁ CR (mm/yr)	0.1848	0.177	7.207	
	B ₂ CR (mm/yr)	0.2233	0.146	0.770	
	B ₃ CR (mm/yr)	0.3619	0.3003	0.708	
	B ₄ CR (mm/yr)		0.3156	0.9303	1.826
	B ₅ CR (mm/yr)		0.2819	0.8307	1.042
	B ₆ CR (mm/yr)		0.1592	0.3669	0.881